Environmental Science: Atmospheres

ROYAL SOCIETY OF CHEMISTRY

PAPER

View Article Online
View Journal | View Issue

Cite this: *Environ. Sci.: Atmos.*, 2026, **6**, 736

Glow discharge induced reactions in mixtures of ozone and chlorodifluoromethane with atmospheric gases

A. Dorn, *[a] H. Mutaf,[b] R. Orhan,[b] W. Wolff,[c] T. Pfeifer[a] and H. Ahmedov[b]

Received 14th September 2025
Accepted 25th March 2026

DOI: 10.1039/d5ea00113g

rsc.li/esatmospheres

The influence of extraterrestrial particles like cosmic radiation (CR) on the chemistry and ozone density in the Earth's stratosphere is not well investigated and normally neglected in stratospheric chemistry models. Here we present the commissioning of a lab-based apparatus which aims at simulating conditions in the stratosphere in order to get better insight into the reactions induced by the secondary-particle showers from high-energetic CR which can reach low altitudes. Admixtures of ozone and the halocarbon $CHClF_2$ (R22, chlorodifluoromethane) to atmospheric gases (N_2, O_2, Ar) were exposed to a glow discharge in the total pressure regime of a few hPa. According to the mass spectrometric analysis of the gas composition the discharge initiates significant ozone depletion by a factor four in the absence of R22. This depletion is strongly enhanced to two orders of magnitude in the presence of R22. The possible underlying reactions are discussed.

Environmental significance

Atmospheric gas mixtures at pressures in the low hPa range are exposed to glow discharges and analyzed by mass spectroscopy. The aim is to simulate stratospheric pressure conditions and to study how charged particle showers initiated by cosmic radiation can influence, *e.g.* the ozone concentration. A typical halocarbon R22 is introduced and its ozone depleting impact is observed. Presently the influence of extraterrestrial energetic particles on the chemistry and ozone density in the Earth's stratosphere is considered to be negligible and normally neglected in stratospheric chemistry models. On the other hand observations by Lu and Sanche [Q.-B. Lu and L. Sanche, *Phys. Rev. Lett.* **87**, 078501 (2001)] suggest that ozone varies with the cosmic radiation flux. Respective research is relevant and timely.

1. Introduction

There is a long history of research on the processes forming and modifying the ozone layer in the Earth stratosphere and on the ozone depleting influence of man-made halocarbons. The main driving force of the stratospheric ozone chemistry is the solar UV radiation. This radiation penetrates the higher-lying atmospheric layers (mesosphere, thermosphere) and is absorbed by oxygen O_2 and ozone O_3 in the stratosphere.

One question that is presently under debate is the influence of the energetic particle streams which originate from the Sun or from sources outside the solar system on the troposphere and biosphere. There is the solar particle stream (solar wind) from protons and alpha particles reaching energies up to roughly 500 MeV. Further, there is cosmic radiation (CR) which can have higher energies but has lower flux. Most primary and secondary particles are stopped in the ionosphere, which concerns essentially all solar particles. Only particle showers initiated by the more energetic CR (>1 GeV) can reach lower atmospheric layers like the stratosphere. Here ionization rates are up to 100 s^{-1} cm^{-3} and the ion density is around a few thousand cm^{-3}. There are observations that CR influences atmospheric properties such as cloud formation and ozone in the stratosphere.[1] In particular Lu demonstrated that stratospheric ozone concentration varies with the 11-year periodicity of the CR flux.[2] The significance of these observations and the underlying mechanisms are under debate. Lu suggested a reaction model where anthropogenic chlorofluorocarbons (CFC) reaching the stratosphere are efficiently dissociated in reactions with secondary electrons from CR which are trapped on surfaces of stratospheric ice crystals.[3]

On the modelling side there are simulations of the atmospheric ionization density as, *e.g.*, the AtRIS code[4] which is a GEANT4 based simulation of CR induced atmospheric particle showers providing ionization densities as function of the incoming radiation energy and the altitude. This data can be the basis for modelling the atmospheric ion chemistry and the influence of CR showers on the relevant quantities like the ozone column density.

[a]*Max Planck Institute for Nuclear Physics, Heidelberg 69117, Germany. E-mail: dornalex@mpi-hd.mpg.de*
[b]*TÜBİTAK National Metrology Institute (UME), Kocaeli, Gebze, Turkey*
[c]*Physics Institute, Federal University of Rio de Janeiro, Rio de Janeiro, Brazil*

Lab based experimental studies on ionization of atmospheric gas mixtures are scarce. Cacace *et al.*[5] have performed mass-spectroscopic ionization studies on mixtures of ozone and hydrochlorofluorocarbons (HCFCs) diluted in atmospheric gases. They found particular compound ions formed from ozone and HCFC which will be discussed below in relation with the present findings.

The abundant secondary electrons produced by the CR particle showers can be of importance for atmospheric ion chemistry. We aim at providing an experimental means to study the effects of electrons on ozone and the influence of HCFCs under conditions similar to the stratosphere. Therefore, we have set-up a laboratory apparatus consisting of a vacuum chamber that can be filled with controlled mixtures of gases at pressures between 1 and 4 hPa. A glow discharge (GDC) is used to provide a hot electron gas to induce energy transfer collisions like electron attachment, excitation and ionization processes and, thereby, initiate dissociation, radical formation and subsequent chemical processes modifying the gas concentrations.

Inelastic collisions and secondary electron production by CR are induced by high energetic charged particles within the particle showers. Their energy transfer in inelastic collisions with atmospheric molecules most likely is small. The secondary electron energy spectrum is maximal close to zero energy and falling off quickly for increasing energy[6–8] such that for 10 eV secondary electron energy the cross section is about half the cross section for energies below 1 eV. The glow discharge electron energy spectrum also contains mostly low energy electrons in the few eV region which can be described as a non-Maxwellian distribution with a tail to higher energies beyond the ionization energies of the gas.[9,10] While the CR induced electron energy distributions in the stratosphere and in a GDC are certainly not identical both are dominated by low energies below 10 eV. Therefore, the main processes induced in molecular gases like excitation, ionization and electron attachment all with subsequent dissociation and production of reactive species are similar.

In our experiment the evolving gas composition is analyzed by means of mass-spectroscopy. First studies were performed with the atmospheric gases (N_2, O_2) and admixtures of ozone and chlorodifluoromethane ($CHClF_2$) which is the main CFC component in the stratosphere.[11] We observe significant modifications of the gas concentrations and in particular a strong reduction of ozone.

2. Experimental

A scheme of the experimental setup is shown in Fig. 1. The experiments are carried out in a vacuum chamber with 0.4 m diameter and 0.5 m height with around 63 l volume. The gases are admitted with individual flux regulators allowing the adjustment of constant gas flows in a range from 10 to 1000 sccm (standard cubic centimeter per minute, 100 sccm = 1.689 hPa l s^{-1}).

An ozone generator (Fischer 500) is utilized to produce a small ozone admixture to the oxygen flow. During experiments the chamber pressure could be varied between 0.1 hPa and 4 hPa by adjusting the gas pumping speed. At the lower pressure range the chamber is pumped by a turbo-molecular pump with an oil-free scroll backing pump. An upstream adjustable throttle valve is used to regulate the pumping speed of the turbo pump and, therefore, the total chamber pressure. In the higher pressure range the chamber is pumped directly by the scroll pump. To achieve the typical experimental conditions with 2 hPa chamber pressure and gas flows of 100–200 sccm a pumping speed of 0.8–1.6 l s^{-1} is required. Therefore, it takes around 40–80 seconds for a complete turnover of the chamber volume of 63 l.

To induce electron-molecule collisions a glow discharge (GDC) is initiated between a cathode and an anode, both with 5 cm diameter and being 7 cm apart. Typical electrical voltages and currents at 2 hPa pressure are 700 V and 10 mA.

The plasma properties are determined by a commercial Langmuir probe (Impedans plasma measurement). Here a voltage biased tungsten wire-tip is introduced into the plasma. By analyzing measured current–voltage (I–V) characteristic curves generated as different voltages are applied to the probe the electron density, the electron temperature and the plasma potential are determined (see, *e.g.*, 12 and 13). The electron gas parameters showed typical electron temperatures between 5 eV and 10 eV and electron densities in the range of $(5–10)\cdot10^7$ cm^{-3}.

2.1 Mass spectrometer

The gas composition at the edge of the plasma region is analyzed with quadrupole mass spectrometer (MS) Pfeiffer QMA200. It is placed in a separate differentially pumped chamber with a 30 cm long nozzle from PTFE material that can be moved close to or into the plasma region and allows gas to enter the MS chamber through an aperture of about 0.3 mm. At the entrance of the MS there is an ion source where the gas is ionized by an electron beam with 60 eV energy and the resulting fragment ions produced are mass analyzed. Therefore, the MS probes essentially the neutral molecules which diffuse into the MS chamber by recording their fragment ion mass spectra. Ions from the plasma will largely neutralize, *e.g.* on surfaces or with electrons on the way to the MS. The neutral molecules reaching the MS can be identified from their known fragmentation patterns into daughter ions.

In the present study we performed full mass scans from 5 to 84 amu for some specific gas mixtures and we measured time lapses tracking the concentrations of the main gas components while varying the GDC and R22 admission. In the latter case only particular fragment ion masses characteristic for the parent molecules of interest were tracked. These are listed in Table 1. *E.g.* R22 ($CHClF_2$) shows various ionic fragments in the mass spectrum with the most abundant one being CHF_2^+ (m/z = 51 amu) with about 90% branching ratio (see NIST reference mass spectrum[14]). Ozone was identified according to the line for m/z = 48 amu corresponding to the O_3^+ ion which is produced with well-known cross section and branching ratio.[15] For mixtures of ozone and R22 the contribution of the R22-fragment ion $CH^{35}Cl^+$ (m = 48 amu) with relative abundance of 0.7% of the CHF_2^+-intensity was corrected for. In order to obtain the

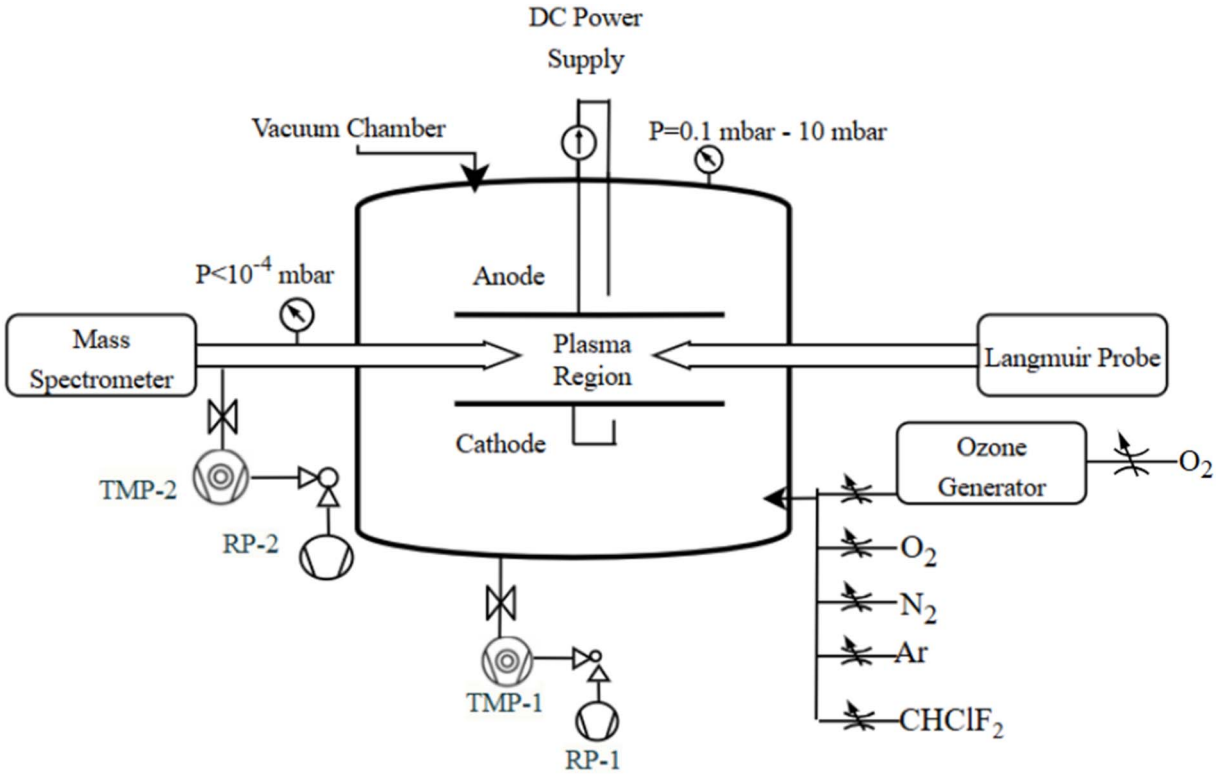

Fig. 1 Scheme of the experimental setup. For details see text.

pure O_3^+ ion signal this contribution was subtracted. Of particular interest in this study were plasma reactions involving R22 and ozone which can form compounds containing oxygen and chlorine. Stable molecules like Cl_2O or Cl_2O_2 which reach the MS ion source were identified by the characteristic $^{37}ClO^+$ ionic fragment ($m/z = 53$ amu). The $^{35}ClO^+$ ion with $m/z = 51$ amu is superimposed and dominated by the CHF_2^+ fragment from R22.

2.2 Ozone generator

The commercial Fischer 500 ozone generator produces ozone by a corona discharge in a stream of ingoing molecular oxygen. For the present conditions the O_3/O_2 ratio reaching the MS was between 1.5% and 2%. Ozone molecules which stick on surfaces where they can react with each other convert to oxygen molecules. Therefore, the differentially pumped MS nozzle was made from Teflon (PTFE) which has a low sticking coefficient for ozone such that the ozone concentrations measured by the MS should come close to the ozone concentration in the plasma region. Since the flow meter measured the total flow of oxygen and ozone going into the reaction chamber, the O_3/O_2 ratio was deduced using the MS from the measured relative ion currents for O_3^+ and O_2^+ and the partial ionization cross sections to produce O_2^+ from O_2, as well as O_3^+ from O_3.[15] In this analysis, the O_2^+ current contribution produced by dissociative ionization of O_3 was found to be a negligible correction.

3. Results

In this study mixtures of atmospheric gases including ozone were exposed to electron collisions in a GDC. Small

Table 1 Atomic/molecular species for which time scans of their concentrations were recorded (column 1). The daughter ions produced in the MS ion source (column 2) and their mass over charge (m/z, column 3) which were used to identify the molecule in the recorded m/z spectra. Column 4 shows the branching ratio for fragmentation into this channel. The last column lists other ions with the same m/z ratio

Gas species	Ion species used for identification	m/z (amu)	Fraction of fragment channel	Other ions with the same m/z
N_2	N_2^+	28	91%	—
O_2	O_2^+	32	91%	—
O_3	O_3^+	48	50%	$CH^{35}Cl^+$
$CHClF_2$ (R22)	CHF_2^+	51	90%	$^{35}ClO^+$
Ar	Ar^+	40	95%	—
^{37}ClO	$^{37}ClO^+$	53	—	—

contributions of hydrochlorofluorocarbon R22 ($CHClF_2$) were introduced which is known to be harmful for ozone in the stratosphere. The MS ion currents are recorded for GDC switched on and off and with R22 flux on and off. Full mass spectra covering all mass over charge ratios m/z between 5 amu and 89 amu can be found in Fig. 2 and between 5 amu and 84 amu in Fig. 3.

Fig. 2 shows the mass spectrum for R22 at low pressure of 0.05 hPa with GDC on and off. The spectra for both cases are rather similar and can be mostly understood from dissociative ionization of $CHClF_2$ in the ion source of the MS plus some residual gas lines from N_2, O_2 and H_2O. Also heterogenous reactions on surfaces, *e.g.*, with adsorbed molecules like water or the admitted gas species can evolve. Significant changes for GDC on are the increase of hydrogen chloride HCl ($m/z = 36, 38$) and HF ($m/z = 20$) which are direct dissociation products of R22. The main ionization channel results in CHF_2^+ ($m/z = 51$) and neutral Cl. At sufficient chamber pressure Cl can form Cl_2 in three-body collisions Cl + Cl + M → Cl_2 + M. Here M is a third collision partner taking energy to stabilize Cl_2. Despite the low pressure of 0.05 hPa the respective ions are found at m/z being 70, 72 and 74 with their characteristic ratios of isotopic line intensities $I(^{35}Cl^{35}Cl^+)/I(^{37}Cl^{35}Cl^+)/I(^{37}Cl^{37}Cl^+)$ = 9/6/1. Also doubly charged $^{35,37}Cl^{2+}$. Show up at mass over charge ratios 17.5 and 18.5.

In Fig. 3 a mass spectrum for 400 sccm flux of O_2, 7 sccm O_3 and 11 sccm of R22 resulting in a chamber pressure of 2.4 hPa is shown. Again m/z spectra with and without GDC are shown and for comparison also the m/z-spectrum without R22 and GDC off. While the flux of R22 is the same as for Fig. 2 the Cl_2 production becomes more significant due to increased probability of three-body collisions at the higher pressure of 2.4 hPa. Furthermore, reaction products from R22 dissociation products and oxygen/ozone are formed. This is indicated by $^{37}ClO^+$ at $m/z = 53$ (^{35}ClO is merged with CHF_2^+ at $m/z = 51$) as well as F_2O^+ ($m/z = 54$)[16] and possibly CFO^+ at $m/z = 47$. Due to their reactivity these radicals will barely reach the MS but react quickly in the plasma. *E.g.*, ClO can bind to another ClO or to a chlorine radical and form the stable molecules Cl_2O_2 or Cl_2O, respectively. When these molecules reach the MS ion source the observed ClO^+ ions and other ionic species are formed (for Cl_2O, see the NIST reference mass spectrum[17]). As in Fig. 2 the GDC increases the HCl^+ and HF^+ intensities. Ozone as seen in the intensity for O_3^+ at $m/z = 48$ is significantly decreasing with R22 flux and with GDC on. Without GDC there is a very small reduction in this line intensity for R22 switched off which is due

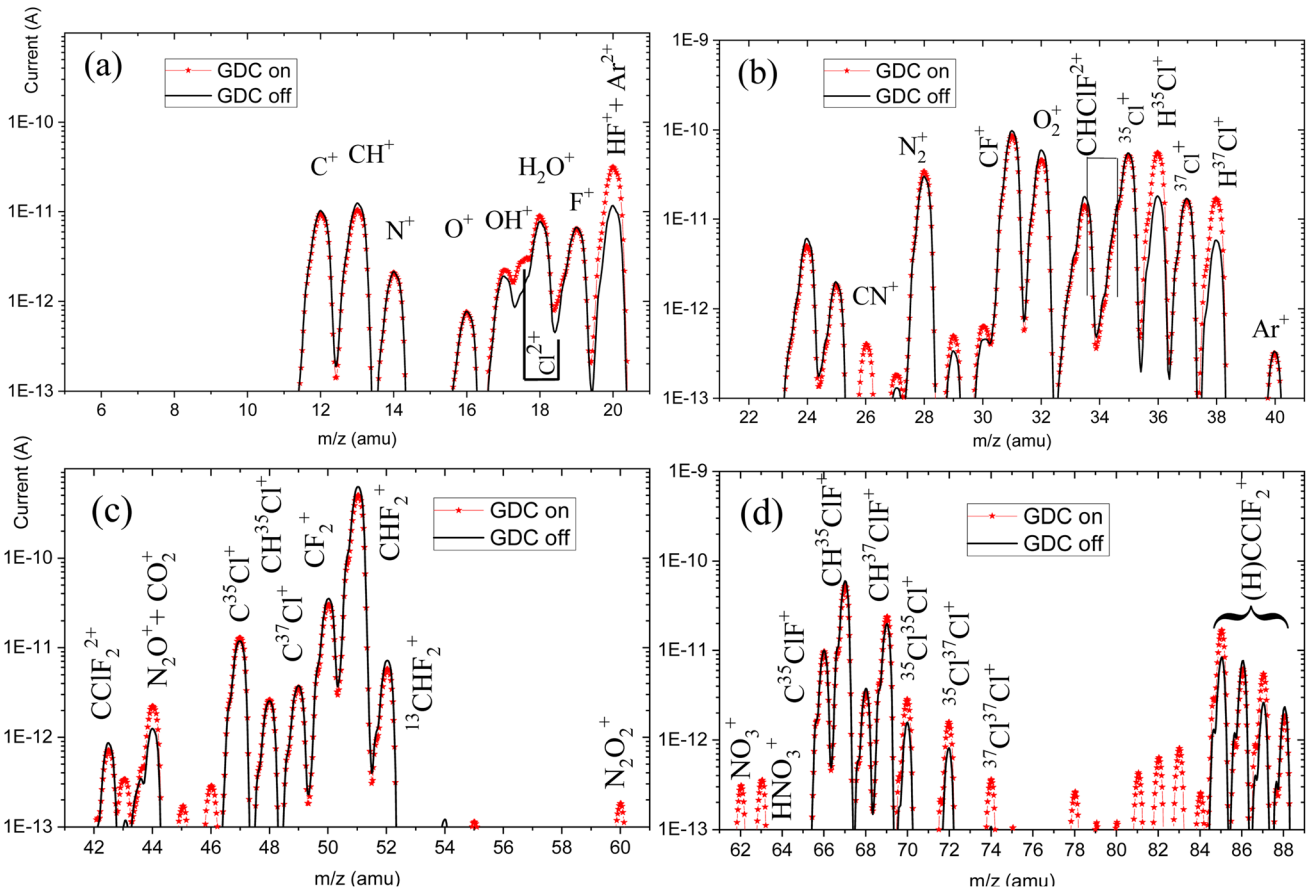

Fig. 2 Full mass scan for R22 flux of 11 sccm corresponding to 0.05 hPa pressure. Measurement with glow discharge (GDC) on (red symbols) and off (black solid line). (a)–(d) show different successive mass ranges.

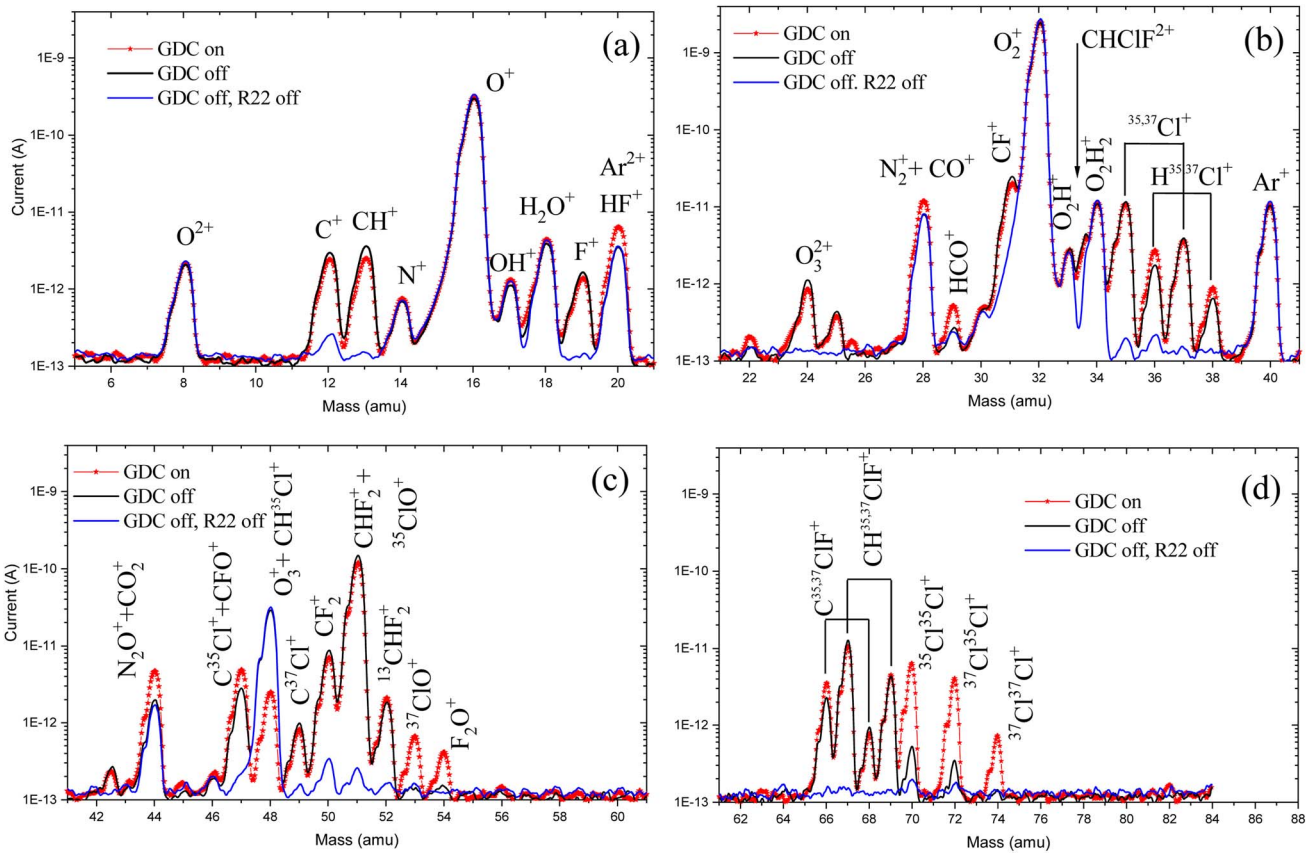

Fig. 3 Mass over charge spectrum for the 400 sccm flux of O_2, 7 sccm O_3 and 11 sccm of R22 at the total pressure 2.4 hPa. Data are shown for glow discharge (GDC) on (red symbols) and off (black line) as well as for R22 flow and GDC switched off (blue line). (a)–(d) show different successive mass ranges. Some lines are due to residual gas components like H_2O^+, OH^+, N_2^+ and N^+.

to a small contribution from the R22 fragment $CH^{35}Cl^+$ (m/z = 48) produced in the MS ion source.

In the following we focus on the behavior of the main gas components in time lapses where we adjust the different gas fluxes. In Fig. 4 an exemplary experimental sequence is presented. The ion yield currents taken with the MS are shown as a function of time. The initial gas flows were N_2: 200 sccm, O_2: 100 sccm and O_3: 1.5 sccm. The shown sequence is an excerpt of a longer measurement where the R22 flux was switched of at time $t = -80$ s. Therefore, the CHF_2^+ current initially still decreases with time. At t_1 the GDC is started (voltage 900 V, current 10 mA). The electron gas temperature was around 6.5 eV and the electron density about $5 \cdot 10^7$ cm^{-3}. A significant reduction of O_3 concentration by a factor of four is observed. In the same time a small increase of the O_2^+ signal of 1.6% is found. After switching off the GDC at t_2 the O_3^+ ion current recovers to the original value. Subsequently at t_3 the $CHClF_2$ gas is admitted with a low flux of 11 sccm which is 3.7% of the combined N_2 and O_2 fluxes. At t_4 the glow discharge is switched on and this results in a strong decrease of ozone by more than two orders of magnitude. Again, there is a small increase of the O_2^+ signal by 1.1%. In the same time also the $CHClF_2$ concentration is reduced by about 15%. Then at t_5 the R22 gas flux is stopped allowing the ozone ion yield to recover to the original

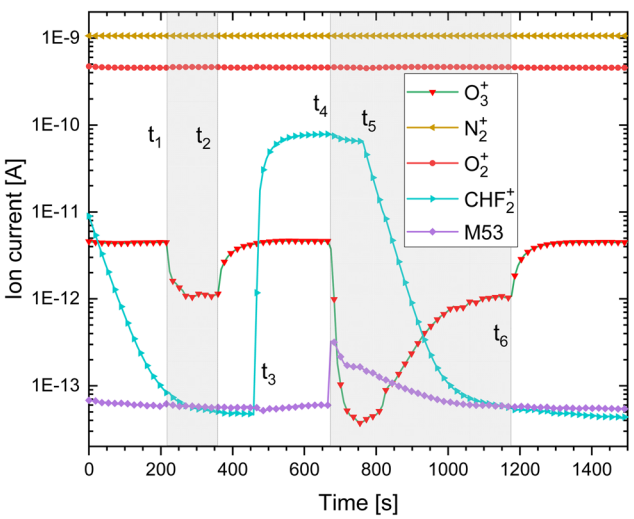

Fig. 4 Experimental ion current variations as function of time for gas fluences of 200 sccm N_2 (M = 28 amu), 100 sccm O_2 (M = 32 amu), 1.5 sccm O_3 (M = 48 amu). Times with GDC operation are shaded in light blue. At times t_1–t_6 the parameters are changed as follows: t_1, t_4: discharge on. t_2, t_6: discharge off. t_3: R22 flux on (11 sccm). t_5: R22 flux off. The total pressure is 1.8 hPa. The data are a section of a longer time lapse during which the R22 flux was switched off at $t = -80$ s. Therefore, a decaying ion current is seen for CHF_2^+ up to t_3.

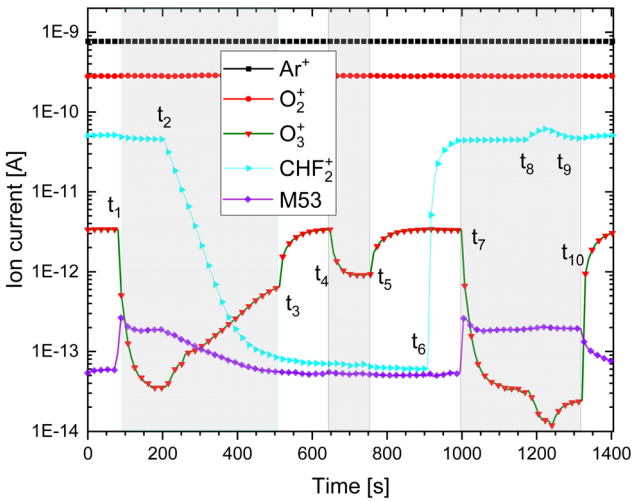

Fig. 5 Experimental ion current variations as function of time with gas fluences of 200 sccm Ar, 100 sccm O_2, 1.9 sccm O_3, 11 sccm R22. Times with GDC operation are shaded in light blue. At times t_1–t_{10} the parameters are changed as follows: t_1, t_4, t_7 GDC on. t_3, t_5, t_{10} GDC off. t_2: R22 flux off. t_6: R22 flux on. Between t_8 and t_9 the R22 flux was slightly increased. The total chamber pressure is 3 hPa.

value for GDC operation which was also found between t_1 and t_2. Finally, when the GDC was stopped at t_6 the ozone concentration settles at the starting value. Additionally, an important observation is the course of the ion with $M = 53$ amu. In the stratosphere the relevant mechanism for ozone depletion by CFCs is the release of chlorine initiating the odd chlorine catalytic cycle which involves ClO as the first product (see discussion below). Therefore, we examined mass 53 corresponding to ^{37}ClO (25% abundance) while ^{35}ClO (75% abundance) is hidden under the dominant peak with $M = 51$ from CHF_2^+. Indeed, there is significant increase in 53 amu yield under plasma operation if both O_3 and R22 flux are on. This leads us to the tentative conclusion that $M = 53$ amu is a reaction product of both molecules where at least one fragment from an electron induced dissociation is involved.

In the stratosphere important ozone depleting reactions involve the odd nitrogen family NO_x (defined as the sum of N, NO, and NO_2).[18] Potentially such species could be produced also in the present N_2/O_2 mixture as a result of the GDC. In order to test if reactions involving ionization or dissociation of N_2 play a role in the observed ozone depletion another experiment was conducted with N_2 replaced by argon (Fig. 5). Initially Ar, O_2, O_3 and R22 gas fluxes were on and at t_1 the discharge was started giving rise to a decrease of ozone by two orders of magnitude. At t_2 R22 was shut off resulting in ozone increase. At t_4 and t_5 the GDC is switched on and off again, respectively, showing ozone decrease by a factor of 3.5. The dependence of the ozone concentration on R22 flux is demonstrated during discharge operation t_7–t_{10} where R22 is briefly increased between t_8 and t_9. This results in a further decline of ozone.

These sequences demonstrate the strong influence of electron collision induced processes on the ozone concentration.

4. Discussion

There are different chemical processes known to evolve in atmospheric gas mixtures with ozone-depleting substances under the influence of ultraviolet radiation or under charged particle impact as in the present case. The basic reaction cycle responsible for ozone production/destruction and the absorption of UV-light is the Chapman cycle:

Ozone production

$$O_2 + h\nu\ (\lambda < 242.4\ \text{nm}) \rightarrow 2O \Rightarrow O + O_2 \xrightarrow{M} O_3 \quad (1)$$

Ozone destruction

$$O_3 + h\nu\ (\lambda < 320\ \text{nm}) \rightarrow O + O_2 \Rightarrow O_3 + O \rightarrow 2O_2 \quad (2)$$

Here M in eqn (1) refers to a third molecule which has to take away the excess energy for stabilization of O_3. In principle both reaction sequences can also be induced in the glow discharge where electron collisions can initiate the molecular excitation steps in (1) and (2). Reactions (2) are the most likely processes for ozone depletion in our study if R22 is absent. This is indicated by the O_2^+ ion current increase, which is consistent with the respective ozone decrease within the accuracy of the measurement. While in the stratosphere there is an equilibrium of O_3 production and O_3 destruction we observe significant stronger discharge-induced destruction. This is due to two reasons. Firstly, the present pressure conditions in the hPa range which is about a factor of ten lower than in the stratosphere. Since the rate of the second step in reaction (1) where a third particle M is required to stabilize O_3 scales with the particle density to the power of three we observe a lower ozone production rate than in the stratosphere. Secondly, the equilibrium ozone concentration in the stratosphere is about a factor of 500 lower than in the present case ($[O_3] \approx 10$ ppm at 23 km altitude) such that ozone dissociation is expected to dominate in our experiment. In addition to the dissociative excitation of reaction (2) other possible electron induced reactions with ozone are ionization ($E > 12.53$ eV) and ionization with subsequent dissociation ($E > 12.8$ eV) producing O_2^+ or O^+.[15] Finally, the more abundant low energy electrons in the glow discharge can undergo dissociative electron attachment (DEA) with ozone between 0 and 3 eV energy yielding O_2^- and O^-.[19] The negative ions can neutralize in collisions with positive ions or surfaces and an effective ozone depletion takes place.

If R22 is introduced a number of new fragments are produced from collisions involving free electrons. The possible reactions are dissociative electron attachment (DEA),[20] dissociative excitation[21] and dissociative ionization.[22] In all these processes the most likely product is the chlorine atom or the negative chlorine ion together with the molecular fragment $CHF_2^{(+)}$. For ionization we have measured the absolute partial ionization cross sections for various CFCs including R22 from low to high impact energies.[23] The dominant fragmentation results in CHF_2^+ + Cl which is also the channel used for detection of R22 according to Table 1. Chlorine in the stratosphere is very efficient in ozone depletion which evolves in catalytic

cycles. In the odd chlorine cycle the following reactions take place.

$$Cl + O_3 \rightarrow ClO + O_2 \quad (3)$$

Followed by

$$ClO + O \rightarrow O_2 + Cl. \quad (4)$$

In our experiment there are signatures that at least the first step of this cycle is playing a significant roll due to the detection of $^{37}ClO^+$ ($M = 53$ amu) in the mass spectrum. As mentioned above these radicals can further react to stable molecules which can reach the MS and give rise to the $^{37}ClO^+$ fragment ion. The rate of the second step depends on the concentration of O which can be produced in electron collisions with O_3 and O_2 analogous to eqn (1) and (2).

Another ozone-depleting reaction in the stratosphere is the odd nitrogen cycle involving NO and NO_2:

$$NO + O_3 \rightarrow NO_2 + O_2 \quad (5)$$

$$O + NO_2 \rightarrow NO + O_2 \quad (6)$$

In the stratosphere the nitrogen oxides mainly originate from nitrous oxide N_2O coming from the troposphere but partially also from CR which ionizes and dissociates N_2 into radicals which further react with O_2.[24] In principle ionization/dissociation of N_2 can also be a source of nitrogen oxides in our experiment. Therefore, we have replaced the N_2 gas by argon and an exemplary experimental sequence is shown in Fig. 5. We found within the accuracy of the MS data the same behavior of the ozone concentration as with nitrogen gas. For GDC operation and with R22 gas supply the ozone reduction is two orders of magnitude while for absence of R22 the ozone concentration is reduced by a factor four. Therefore, the nitrogen oxides do not seem to play a significant role in the present experiment. One reason might be the large N_2 binding energy of 9.7 eV in combination with the relatively low temperature of the electron gas which results in a low N_2 dissociation rate. It should be mentioned that the full mass scans in Fig. 2 and 3 show small line intensities with possible assignments to nitrogen oxides like NO^+ ($M = 30$ amu), NO_2^+ ($M = 46$) and N_2O^+ ($M = 44$). They can originate from reactions with ionization/dissociation products of residual nitrogen gas which shows up in the lines N_2^+ ($M = 28$) and N^+ ($M = 14$).

Another ozone depleting mechanism was found in a previous study by Cacace *et al.*[5] using advanced analytical and mass spectroscopic methods. The authors have found reactions between ionized ozone and CFCs which in case of R22 are:

$$O_3^+ + CHClF_2 \rightarrow CHF_2O_3^+ + Cl \quad (7)$$

Here the ion is unstable and its main fragmentation channel is producing neutral CO.

$$CHF_2O_3^+ \rightarrow HF_2O_2^+ + CO \quad (8)$$

CO with $M = 28$ has the same mass as N_2 such that we cannot separate it with the present MS. Nevertheless, in the mass scan of Fig. 3 for a mixture of 400 sccm O_2, 7 sccm O_3 and 11 sccm R22 we find that the initial $M = 28$ amu peak intensity due to residual N_2 gas increases for GDC operation by around 50%. The $M = 28$ amu peak is unchanged with/without discharge if R22 is not introduced. Therefore, a certain quantity of CO is produced from reactions like eqn (7) and (8). In the full mass scans we found indications of more reaction products from ozone and R22 which are initiated by the discharge like F_2O^+ ($M = 54$ amu). This supports the findings of Cacace *et al.* that there is a rich chemistry between ions and neutrals of oxygen, ozone and F22.

In order to conclude on processes in the Earth's stratosphere several aspects have to be considered. In the stratosphere the ionization density by CR is much lower than in the glow discharge, namely around 10–100 cm^{-3} s^{-1} and the resulting electron-ion pair density is around 10^3–10^4 cm^{-3}. In comparison the electron-ion density in the present experiment is above 10^7 cm^{-3}. Therefore, the present experiment strongly enhances the collisional reactions in the gas mixture. On the other hand, the catalytic ozone depleting cycles are running on longer time scales and cannot contribute significantly to modify the ozone concentrations due to the fast gas exchange rate in the present experiment. From these observations possible future studies should aim at higher chamber pressure of 10 to 20 hPa and lower gas turnover rates to better mimic stratospheric conditions. As result of these conditions significantly lower halocarbon concentration would be required to influence ozone concentration.

5. Summary

In conclusion we studied the influence of a glow discharge on mixtures of atmospheric gases (O_2, N_2, Ar) containing ozone and a typical halomethane R22 ($CHClF_2$). The pressure range was a 1–3 hPa in order to come close to conditions in the upper stratosphere. The gas composition was analyzed with mass spectrometry and the electron-gas temperature was in the range of 5–10 eV with densities $5–10 \cdot 10^7$ cm^{-3}. In absence of R22 the discharge initiates ozone depletion by factor of four which is enhanced to two orders of magnitude by addition of about 3% of R22 flux. The possible underlying collisional and chemical processes were discussed. The reactions involving nitrogen do not seem to play a significant role.

Possible future studies should analyze the pressure dependence of the observations. *E.g.* at higher pressure the discharge-induced ozone depletion can be compensated by ozone production in three-body processes $O + O_2 + M \rightarrow O_3 + M$. Also, the gas exchange rate can be reduced in order to enhance the role of the repeating catalytic cycles with respect to the initial collisional processes. In this way the natural stratospheric conditions can be better approached and extrapolations to lower halomethane concentrations and lower electron densities can be performed. In addition, modelling of the atmospheric chemical processes starting from the various collisional reactions initiated by low energetic electrons would be desirable.

Conflicts of interest

There are no conflicts to declare.

Data availability

All data supporting our findings are included in the main article.

Acknowledgements

The project 21GRD02 BIOSPHERE has received funding from the European Partnership on Metrology, co-financed by the Horizon Europe Research and Innovation Program of the European Union and the participating States. Funder ID: 10.13039/100019599. Grant number: 21GRD02 BIOSPHERE. Open Access funding provided by the Max Planck Society.

References

1 (*a*) H. Svensmark and E. Friis-Christensen, *J. Atmos. Terr. Phys.*, 1997, **59**, 1225; (*b*) H. Svensmark, *Phys. Rev. Lett.*, 1998, **81**, 5027; (*c*) N. D. Marsh and H. Svensmark, *Phys. Rev. Lett.*, 2000, **85**, 5004.
2 Q. B. Lu and L. Sanche, *Phys. Rev. Lett.*, 2001, **87**, 078501.
3 Q.-B. Lu, *AIP Adv.*, 2021, **11**, 115307, DOI: 10.1063/5.0047661.
4 S. Banjac, K. Herbst and B. Heber, *J. Geophys. Res. Space Phys.*, 2019, **124**, 50.
5 (*a*) F. Cacace, G. de Petris, F. Pepi, M. Rosi and A. Troiani, *Chem. Eur J.*, 2000, **6**, 2572; (*b*) F. Cacace, G. de Petris, F. Pepi, M. Rosi and A. Sgamellotti, *Angew. Chem., Int. Ed.*, 1999, 2408.
6 C. B. Opal, W. K. Peterson and E. C. Beaty, *J. Chem. Phys.*, 1971, **55**, 4100.
7 M. E. Rudd, *Phys. Rev. A*, 1988, **38**, 6129.
8 K. Kiyohara, *et al.*, *Prog. Nucl. Sci. Technol.*, 2011, **1**, 222.
9 M. Venugopalan, *Nucl. Instrum. Methods Phys. Res., Sect. B*, 1987, **23**, 405, DOI: 10.1016/0168-583X(87)90467-8.
10 M. J. Druyvesteyn and F. M. Penning, *Rev. Mod. Phys.*, 1940, **12**, 87, DOI: 10.1103/RevModPhys.12.87.
11 S. A. Montzka, B. D. Hall and J. W. Elkins, *Geophys. Res. Lett.*, 2009, **36**, L03804.
12 B. E. Cherrington, *Plasma Chem. Plasma Process.*, 1982, **2**, 113, DOI: 10.1007/BF00633129.
13 W. P. S. Tan, *J. Phys. D: Appl. Phys.*, 1973, **6**, 1206.
14 NIST Chemistry WebBook, https://webbook.nist.gov/cgi/cbook.cgi?ID=C75456&Units=SI&Mask=200#Mass-Spec.
15 K. A. Newson, S. M. Luc, S. D. Price and N. J. Mason, *Int. J. Mass Spectrom. Ion Processes*, 1995, **148**, 203.
16 J. Berkowitz, P. M. Dehmer and W. A. Chupka, *J. Chem. Phys.*, 1973, **59**, 925, DOI: 10.1063/1.1680115.
17 NIST Chemistry WebBook, https://webbook.nist.gov/cgi/cbook.cgi?ID=C7791211&Units=SI&Mask=200#Mass-Spec.
18 B. A. Thrush, *Phil. Trans. Roy. Soc. Lond. Math. Phys. Sci.*, 1980, **296**, 149, DOI: 10.1098/rsta.1980.0161.
19 G. Senn, J. D. Skalny, A. Stamatovic, N. J. Mason, P. Scheier and T. D. Märk, *Phys. Rev. Lett.*, 1999, **82**, 5028.
20 P. Cicman, A. Pelc, W. Sailer, S. Matejcik, P. Scheier and T. D. Märk, *Chem. Phys. Lett.*, 2003, **371**, 231.
21 J. F. Ying and K. T. Leung, *J. Chem. Phys.*, 1996, **105**, 2188–2198, DOI: 10.1063/1.472092.
22 L. S. N. Ferreira, L. H. Coutinho, V. L. B. de Jesus and E. C. Montenegro, *J. Phys. B:At., Mol. Opt. Phys.*, 2012, **45**, 215203.
23 (*a*) M. Dogan, W. Wolff, D. M. Mootheril, T. Pfeifer and A. Dorn, *Phys. Chem. Chem. Phys.*, 2025, **27**, 10057; (*b*) W. Wolff, M. Dogan, H. Luna, L. H. Coutinho, D. Mootheril, W. Baek, T. Pfeifer and A. Dorn, *Rev. Sci. Instrum.*, 2024, **95**, 095103.
24 M. Nicolet, *Planet. Space Sci.*, 1975, **23**, 637.